Enhanced Characterization of Cardiolipins via Hybrid 193 nm Ultraviolet Photodissociation Mass Spectrometry

Luis A. Macias and Jennifer S. Brodbelt*

Department of Chemistry, The University of Texas at Austin, Austin, TX, 78712

Supporting Information

Supplementary Methods

Materials. CL standards, PG standards, and *E.coli* CL were purchased from Avanti Polar Lipids (Alabaster, Alabama). Molecular weights and structures for PG and CL standards are shown in **Table S1**. Sodium acetate, (trimethylsilyl)diazomethane (TMSD), HPLC grade water, and HPLC grade methanol were obtained from EMD Millipore (Billerica, MA). Chloroform was obtained from Sigma-Aldrich (St. Louis, MO). Methyl tert-butyl ether (MTBE) was obtained from Alfa Aesar (Haverhill, MA). A total lipid extract was prepared from a papillary thyroid carcinoma obtained from the Cooperative Human Tissue Network using a Bligh and Deyer lipid extraction protocol.[1] Prior to electrospray ionization, samples were prepared in a 50:50 methanol/chloroform solution doped with 1 mM sodium acetate at a final concentration of 2-10 µM for CL and PG standards and 10 ng/µL for biological extracts, unless otherwise indicated.

TMSD Methylation of Phospholipids. Phospholipid derivatization via TMSD is described elsewhere[2,2–5] and adapted as follows: for lipid standards and the *E.coli* CL, 1 mg of material was dried out of the stock solution under a stream of nitrogen and resuspended in 500 µL of upper phase of MTBE/methanol/water (100:30:25, v/v) mixture. For the papillary thyroid carcinoma, half of the material produced by the Bligh and Deyer extraction (approximately 1.5 mg) was solvated in 500 µL of the MTBE/methanol/water mixture. To initiate the methylation reaction, 50 µL of 2 M TMSD hexane solution were added to the lipid solution and incubated at room temperature for 20 minutes. The reaction was quenched with 10 µL of glacial acetic acid, producing a visible color change from yellow to clear. The solution was subsequently washed 2x with 500 µL of the lower phase of the MTBE/methanol/water mixture and centrifugation at 1500 g for 3 min. After the final wash, the organic phase was collected in a glass vial, dried down, and reconstituted at 1 mg/mL in chloroform for storage at -20 ºC.

Nomenclature. Lipid shorthand notation was used as described by Liebsich et al.[6] and modified as previously described for CL.[7] Briefly, phospholipid classes are defined by letter abbreviations followed by sum composition or acyl chain composition as indicated by the number of carbons followed by ":" and the degrees of unsaturation. If *sn* regiochemistry is known, fatty acid identities are separated by "/" or otherwise by "_". If a double bond position is known, it is indicated in parentheses followed by Z, E, or Δ, to indicate the geometry as *cis*, *trans*, or unknown, respectively. For CL, PA moiety compositions are indicated in parentheses to inform that the individual identities are known. PA compositions are separated by "/" or "_" to indicate that the chirality of the central glycerol is known or unknown, respectively. For example, CL (16:0/18:0)_(16:0/18:1(9Z)) indicates a CL structure composed of one PA moiety with a 16:0 fatty acid at *sn*-1 position and a 18:0 fatty acid at the *sn*-2 position, coupled to a second PA moiety with a 16:0 at the *sn*-1 position and 18:1 at the *sn*-2 position, where the latter fatty acid incorporates a *cis* double bond between carbon 9 and 10 on the acyl chain.

Table S1. Structure of all standard lipids.

Lipid Name	Lipid Structure	Exact Mass (Da)
1',3'-bis[1-palmitoyl-2-oleoyl-sn-glycero-3-phospho]-glycerol CL (16:0/18:1(9Z))/(16:0/18:1(9Z))	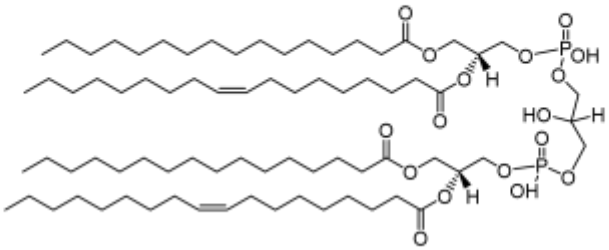	1405.00
1-palmitoyl-2-oleoyl-sn-glycero-3-phospho-(1'-rac-glycerol) PG 16:0/18:1(9Z)	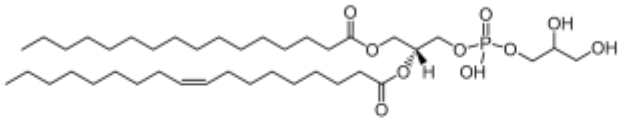	748.53
1-oleoyl-2-palmitoyl-sn-glycero-3-phospho-(1'-rac-glycerol) PG 18:1(9Z)/16:0	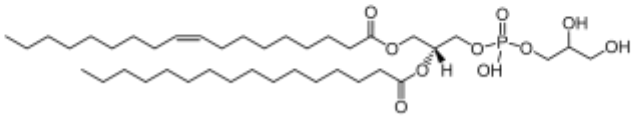	748.53

Table S2. Product ion *m/z* values for HCD/UVPD fatty acid allyl ester fragments of common fatty acids.

Fatty Acid	Allyl ester *m/z*
14:0	291.2295
14:1	289.2138
15:0	305.2451
15:1	303.2295
16:0	319.2608
16:1	317.2451
16:2	315.2295
17:0	333.2764
17:1	331.2608
18:0	347.2921
18:1	345.2764
18:2	343.2608
18:3	341.2451
19:0	361.3077
19:1	359.2921
20:0	375.3234
20:1	373.3077
20:2	371.2921
20:3	369.2764
20:4	367.2608
20:5	365.2451
22:6	391.2608

Table S3. *E. coli* CL structures characterized with *sn*-isomer and double bond resolution.

Precursor (m/z)	HCD			UVPD				Major CL Isomer
	PA + Headgroup + Na (m/z)	PA Moiety Sum Composition	Dioxolane + Na (m/z)	Fatty Acid Allyl Ester (m/z)	sn-stereochemistry	PA Isomer %	Double Bond Fragments (m/z)	
1347.93	825.46	30:0	545.46	319.26	16:0/14:0	91.5		CL (16:0/14:0)_(16:0/14:0)
				291.23	14:0/16:0	8.5		
1371.93	823.45	30:1	543.44	291.23	14:0/16:1	89.6	433.33, 457.33	CL (16:0/16:1(9Δ)_(14:0/16:1(9Δ))
				317.24	16:1/14:0	10.4		
	851.48	32:1	571.47	319.26	16:0/16:1	94.5	461.36, 485.36	
				317.24	16:1/16:0	5.5		
1373.95	825.46	30:0	545.46	319.26	16:0/14:0	89.8		CL (16:0/16:1(9Δ))_(16:0/14:0)
				291.23	14:0/16:0	10.2		
	851.48	32:1	571.47	319.26	16:0/16:1	94.6	461.36, 485.36	
				317.24	16:1/16:0	5.4		
1397.95	849.46	32:2	569.45	317.24	16:1/16:1	-	459.34, 483.34	CL (16:0/16:1(9Δ))_(16:1(9Δ)/16:1(9Δ))
	851.48	32:1	571.47	319.26	16:0/16:1	95.7	461.36, 485.36	
				317.24	16:1/16:0	4.3		
1399.96	851.47	32:1	571.47	319.26	16:0/16:1	95.5	461.36, 485.36	CL (16:0/16:1(9Δ)_(16:0/16:1(9Δ))
				317.24	16:1/16:0	4.5		
1400.97	851.48	32:1	571.47	319.26	16:0/16:1	95.3	461.36, 485.36	CL (16:0/16:0)_(16:0/16:1(9Δ))
				317.25	16:1/16:0	4.7		
	853.49	32:0	573.49	319.26	16:0/16:0	-		
1403.99	853.49	32:0	573.49	319.26	16:0/16:0	-		CL (16:0/16:0)_(16:0/16:0)
1423.96	849.46	32:2	569.45	317.24	16:1/16:1	-	459.34, 483.34	CL (18:1(11Δ)/16:1(9Δ))_(16:1(9Δ)/16:1(9Δ))
	877.50	34:2	597.48	345.27	18:1/16:1	87.7	487.37, 511.37	
				317.24	16:1/18:1	12.3		
1425.98	851.48	32:1	571.47	319.26	16:0/16:1	93.4	461.36, 485.36	CL (18:1(11Δ)/16:1(9Δ))_(16:0/16:1(9Δ))
				317.24	16:1/16:0	6.6		
	877.50	34:2	597.48	345.27	18:1/16:1	88.3	487.37, 511.37	
				317.24	16:1/18:1	11.7		
1427.99	851.48	32:1	571.47	319.26	16:0/16:1	95.3	461.36, 485.36	CL (16:0/18:1(11Δ)_(16:0/16:1(9Δ))
				317.24	16:1/16:0	4.7		
	879.51	34:1	599.50	319.26	16:0/18:1	88.3	489.39, 513.39	
				345.28	18:1/16:0	11.7		
1451.99	877.50	34:2	597.49	345.27	18:1/16:1	87.5	487.37, 511.37	CL (18:1(11Δ)/16:1(9Δ))_(18:1(11Δ)/16:1(9Δ))
				317.24	16:1/18:1	12.5		
1454.01	877.50	34:2	597.49	345.27	18:1/16:1	88.6	487.37, 511.37	CL (18:1(11Δ)/16:1(9Δ))_(16:0/18:1(11Δ))
				317.24	16:1/18:1	11.4		
	879.51	34:1	599.50	319.26	16:0/18:1	92.3	489.39, 513.39	
				345.28	18:1/16:0	7.7		
1456.02	879.51	34:1	599.50	319.26	16:0/18:1	90.4	489.39, 513.39	CL (16:0/18:1(11Δ))_(16:0/18:1(11Δ))
				345.27	18:1/16:0	9.6		
1480.03	877.50	34:2	597.48	345.27	18:1/16:1	89.1	487.37, 511.37	CL (18:1(11Δ)/18:1(11Δ))_(18:1(11Δ)/16:1(9Δ))
				317.24	16:1/18:1	10.9		
	905.53	36:2	625.52	345.27	18:1/18:1	-	515.41, 539.41	
1482.04	879.51	34:1	599.50	319.26	16:0/18:1	89.4	489.39, 513.39	CL (18:1(11Δ)/18:1(11Δ))_(16:0/18:1(11Δ))
				345.28	18:1/16:0	10.6		
	905.53	36:2	625.52	345.27	18:1/18:1	-	515.41, 539.41	

Table S4. PTC CL structures characterized with *sn*-isomer resolution. Isomer percentages are not reported for PA moieties composed of identical acyl chains (i.e. 18:2/18:2) or moieties for which the *sn*-isomer was not identified.

Precursor (*m/z*)	HCD			UVPD			CL Assignments
	PA + Headgroup + Na (*m/z*)	PA Moiety Sum Composition	Dioxolane + Na (*m/z*)	Fatty Acid Allyl Ester (*m/z*)	*sn*-stersochemistry	PA Isomer %	
1500.00	901.50	36:4	621.49	343.26	18:2/18:2	-	CL(18:2/18:2)_(18:2/18:2), CL(18:2/18:2)_(16:0/20:4), CL(18:2/18:2)_(20:4/16:0), CL(16:0/20:4)_(16:0/20:4), CL(20:4/16:0)_(20:4/16:0), CL(16:0/20:4)_(20:4/16:0)
				319.26	16:0/20:4	89.5	
				367.27	20:4/16:0	10.5	
1502.01	901.50	36:4	621.48	343.26	18:2/18:2	-	CL(18:2/18:2)_(18:2/18:1), CL(18:2/18:2)_(18:1/18:2), CL(16:0/20:4)_(18:2/18:1), CL(20:4/16:0)_(18:2/18:1), CL(16:0/20:4)_(18:1/18:2), CL(20:4/16:0)_(18:1/18:2)
				319.26	16:0/20:4	89.7	
				367.28	20:4/16:0	10.3	
	903.51	36:3	623.50	343.26	18:2/18:1	80.6	
				345.28	18:1/18:2	19.4	
1504.02	903.51	36:3	623.50	343.26	18:2/18:1	76.5	CL(18:2/18:1)_(18:2/18:1), CL(18:1/18:2)_(18:1/18:2), CL(18:2/18:1)_(18:1/18:2)
				345.27	18:1/18:2	23.5	
1526.01	901.50	36:4	621.49	343.26	18:2/18:2	-	CL(18:2/18:2)_(18:2/20:3), CL(18:2/18:2)_(20:3/18:2), CL(18:2/18:2)_(18:1/20:4), CL(18:2/18:2)_(20:4/18:1), CL(16:0/20:4)_(18:2/20:3), CL(16:0/20:4)_(20:3/18:2), CL(16:0/20:4)_(18:1/20:4), CL(16:0/20:4)_(20:4/18:1), CL(20:4/16:0)_(18:2/20:3), CL(20:4/16:0)_(20:3/18:2), CL(20:4/16:0)_(18:1/20:4), CL(20:4/16:0)_(20:4/18:1)
				319.26	16:0/20:4	89.6	
				367.28	20:4/16:0	10.4	
	927.51	38:5	647.50	343.26	18:2/20:3	78.1	
				369.27	20:3/18:2	21.9	
				345.27	18:1/20:4	83.0	
				367.26	20:4/18:1	17.0	
1528.03	901.50	36:4	621.48	343.26	18:2/18:2	-	CL(18:2/18:2)_(18:0/20:4), CL(18:2/18:2)_(18:2/20:2), CL(18:2/18:2)_(20:2/18:2), CL(16:0/20:4)_(18:0/20:4), CL(16:0/20:4)_(18:2/20:2), CL(16:0/20:4)_(20:2/18:2), CL(20:4/16:0)_(18:0/20:4), CL(20:4/16:0)_(18:2/20:2), CL(20:4/16:0)_(20:2/18:2)
				319.26	16:0/20:4	89.3	
				367.28	20:4/16:0	10.7	
	929.53	38:4	649.52	347.29	18:0/20:4	-	
				343.26	18:2/20:2	81.8	
				371.29	20:2/18:2	18.2	
1530.04	903.51	36:3	623.50	343.26	18:2/18:1	63.7	CL(18:2/18:1)_(18:0/20:4), CL(18:2/18:1)_(18:2/20:2), CL(18:2/18:1)_(20:2/18:2), CL(18:1/18:2)_(18:0/20:4), CL(18:1/18:2)_(18:2/20:2), CL(18:1/18:2)_(20:2/18:2)
				345.27	18:1/18:2	36.3	
	929.53	38:4	649.52	347.29	18:0/20:4	-	
				343.26	18:2/20:2	84.8	
				371.29	20:2/18:2	15.2	

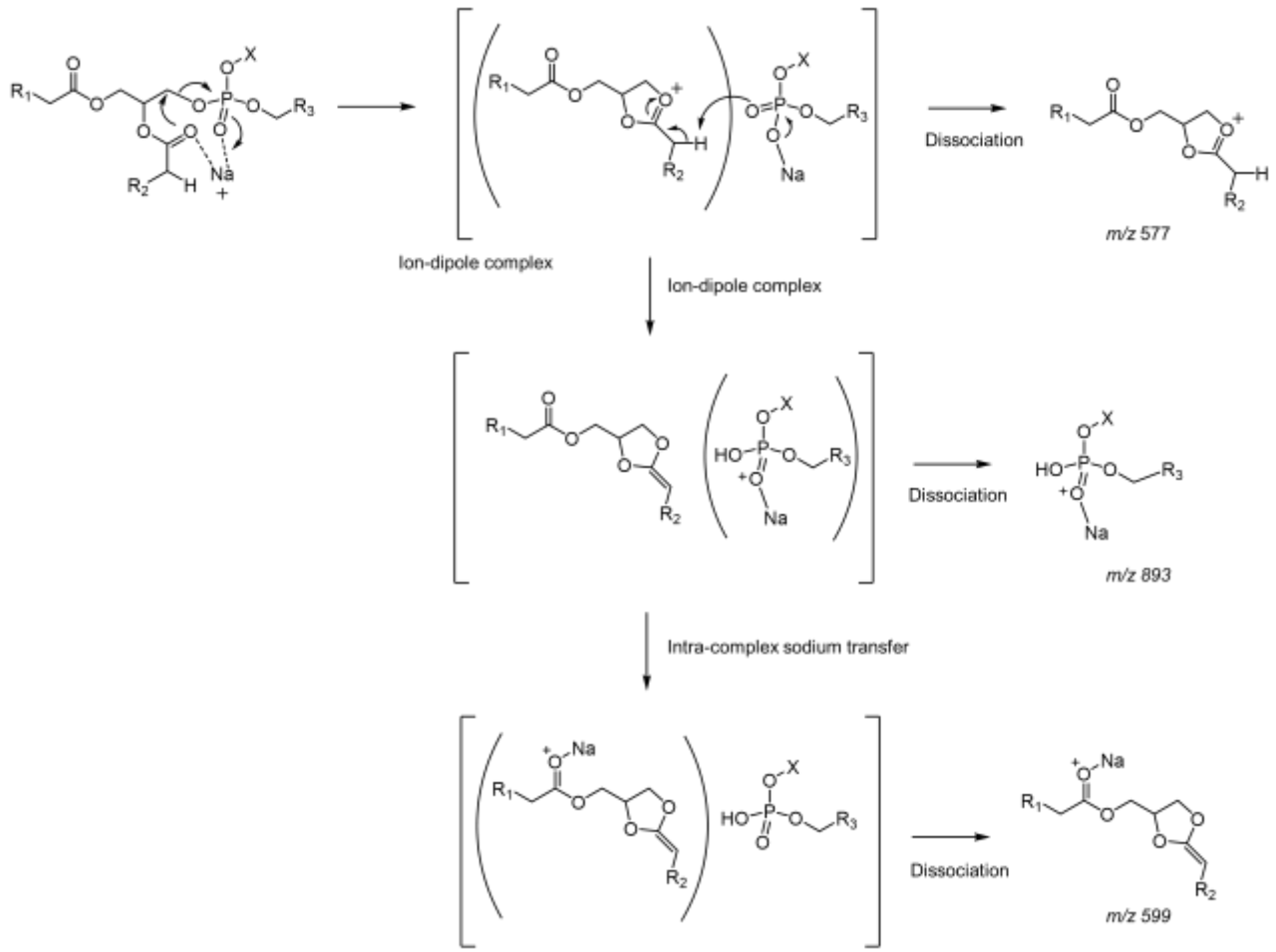

Scheme S1. Fragmentation pathway for dioxolane fragments from metal adducted glycerophospholipids. Fragment *m/z* mass labels correspond to HCD fragment masses in **Figure S1**. Adapted from Ref. 8 and 9.

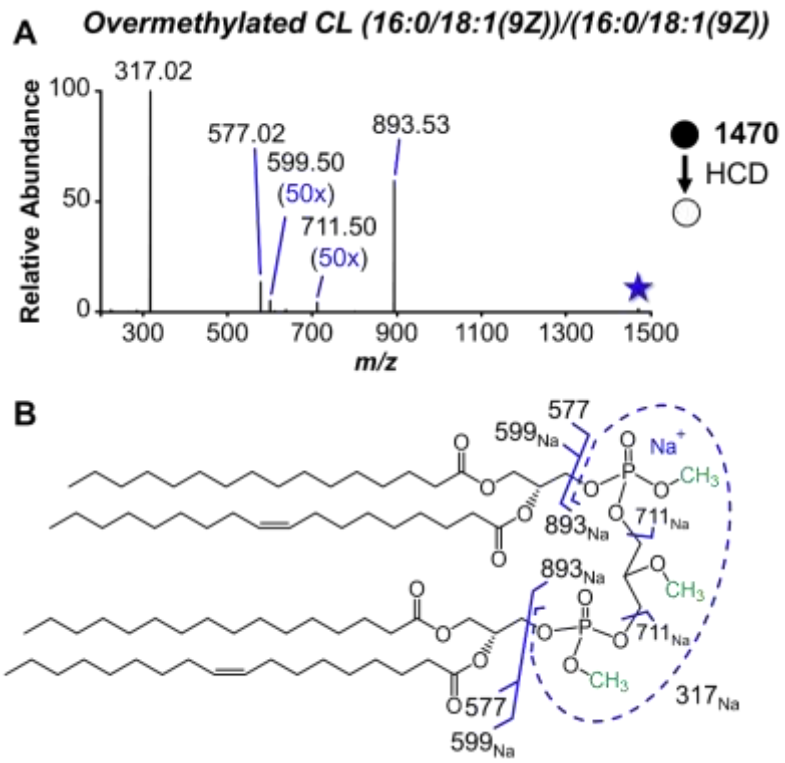

Figure S1. (A) HCD (25 NCE) spectrum of sodium-cationized overmethylated CL (16:0/18:1)/(16:0/18:1) and (B) fragment map. Fragment ions of *m/z* 599.50 and *m/z* 711.49 are shown with 50x magnification. Each selected precursor ion is demarcated with a star.

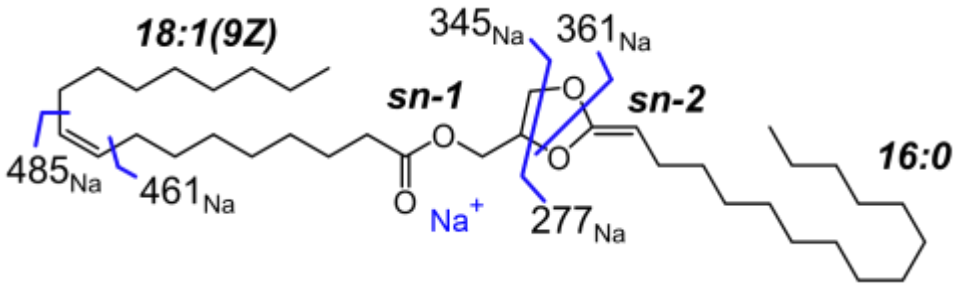

Figure S2. Fragment map for 18:1(9Z)/16:0 dioxolane *sn*-isomer marked with fragments observed in HCD/UVPD spectrum in **Figure 2C**.

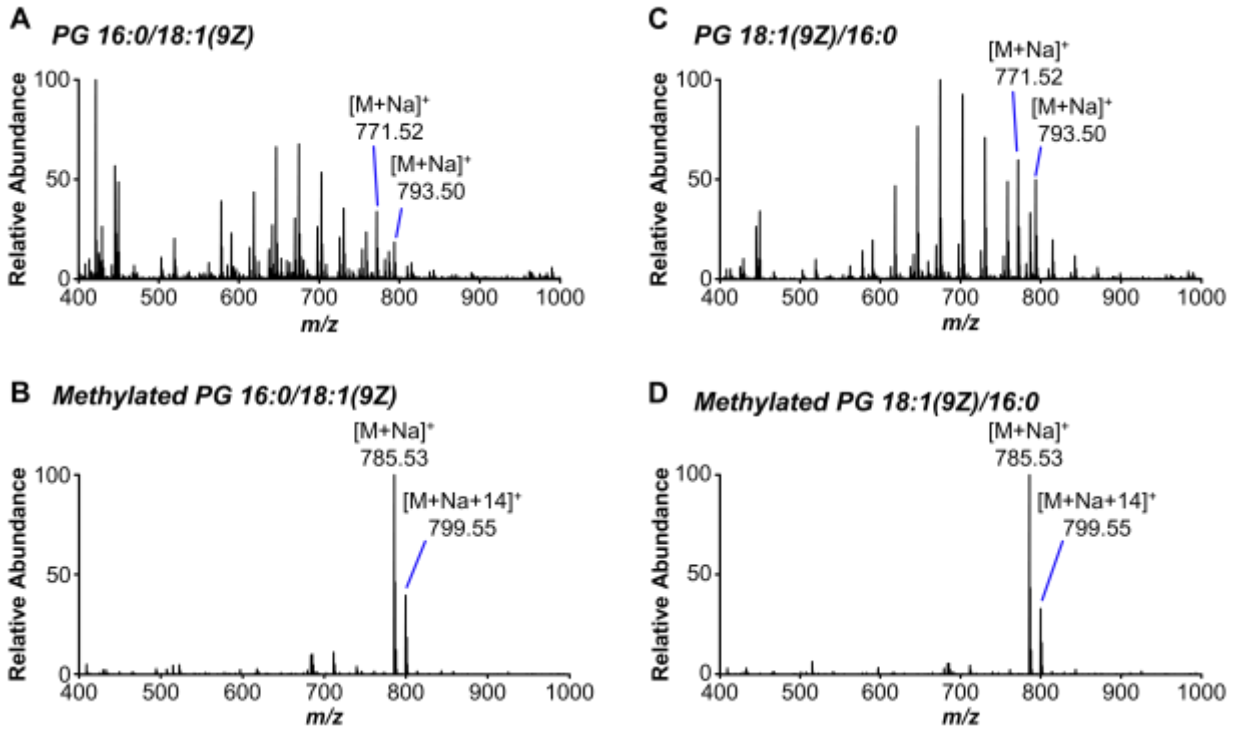

Figure S3. Positive mode nESI spectrum of PG 16:0/18:1(9Z) (A) prior to derivatization and (B) post TMSD methylation. Positive mode nESI spectrum of PG 18:1(9Z)/16:0 (C) prior to derivatization and (D) post TMSD methylation. CID spectra for methylated sodium-cationized ions are shown in **Figure S4**. CID/UVPD spectra are shown in **Figure 3**.

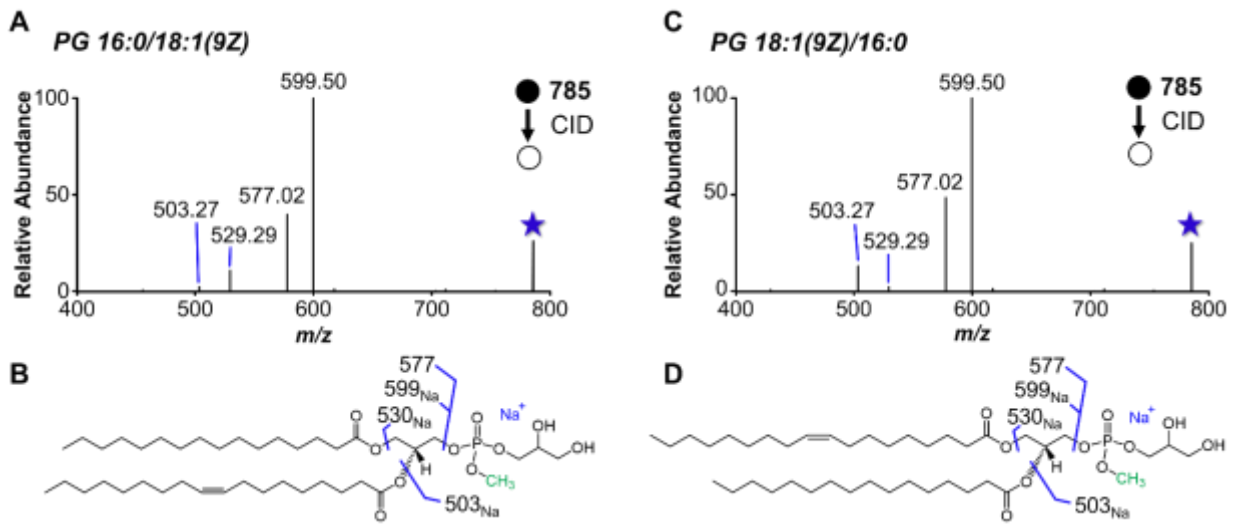

Figure S4. (A) CID (32 NCE) spectrum of sodium-cationized methylated PG 16:0/18:1(9Z) and (B) fragment map. (C) CID (32 NCE) spectrum of sodium-cationized methylated PG 18:1(9Z)/16:0 and (D) fragment map. CID/UVPD spectra are shown in **Figure 3**. Selected precursor ion is demarcated with a star.

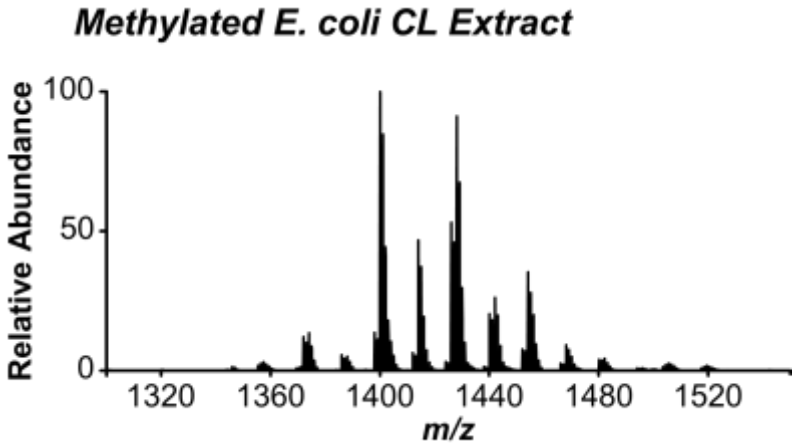

Figure S5. Positive mode MS^1 spectrum of methylated *E. coli* CL extract ionized from solution doped with sodium acetate.

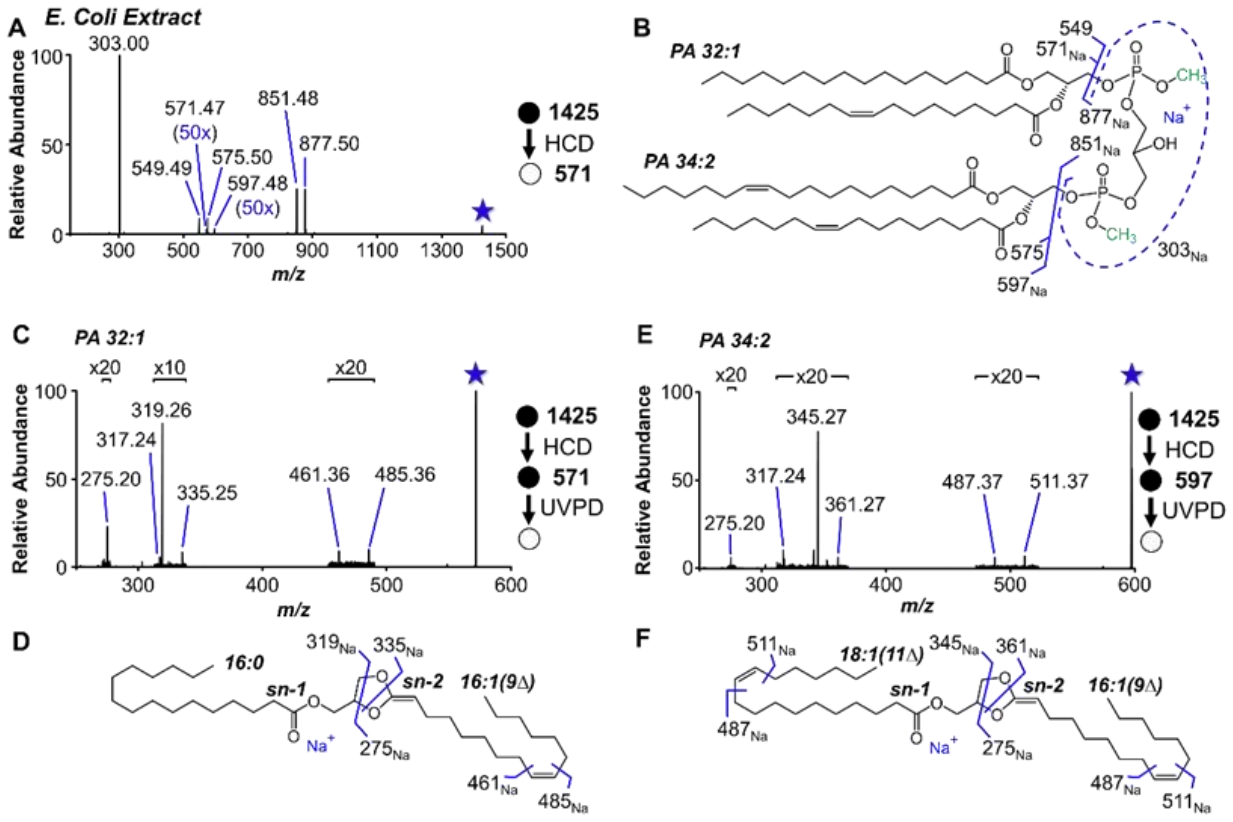

Figure S6. Structural characterization of CL at m/z 1425 from E. coli extract after methylation. (A) HCD (35 NCE) fragments reveal PA moieties PA 32:1 and PA 34:2. Fragments of m/z 571.47 and m/z 597.26 are shown with 50x magnification. (B) HCD fragment map. (C) UVPD (10 pulses at 3 mJ) of headgroup loss fragment from PA 32:1, m/z 571.47, confirms the major structure as PA 16:0/16:1(9Δ). (E) UVPD (10 pulses at 3 mJ) of headgroup loss fragment from PA 34:2, m/z 597.48, confirms the major structure as PA 18:1(11Δ)/16:1(9Δ). Each selected precursor ion is demarcated with a star. Fragment maps constructed from (B) HCD and (D, F) HCD/UVPD elucidate the *E. coli* structure as CL (16:0/16:1(9Δ))_(18:1(11Δ)/16:1(9Δ)) at double bond and acyl chain position level.

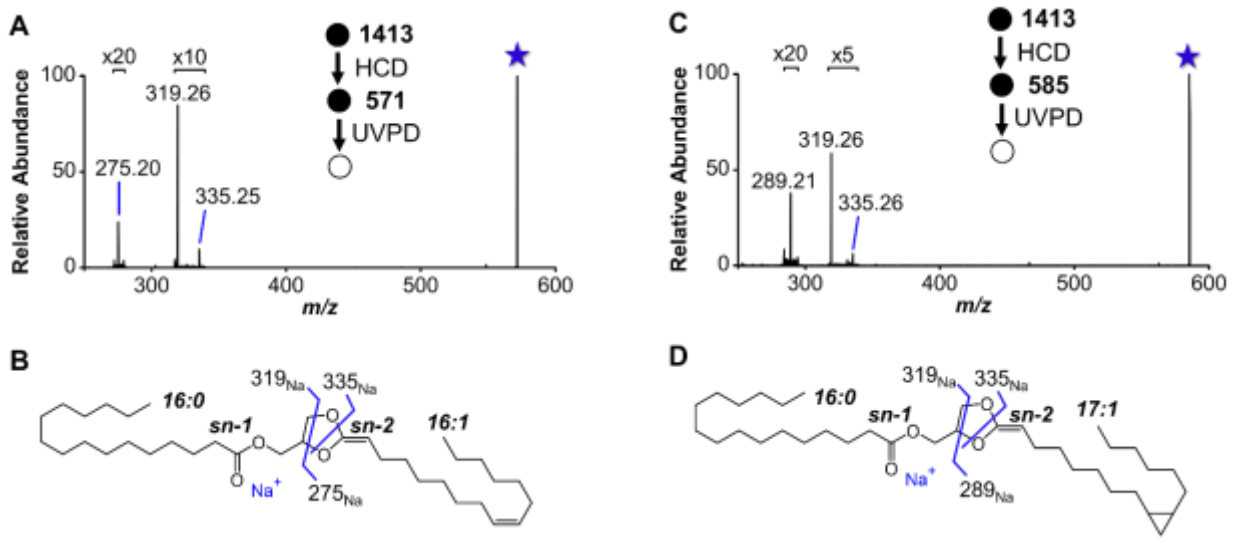

Figure S7. HCD/UVPD analysis of PA moieties from CL 51:2 at *m/z* 1413.98 produced from the methylated *E. coli* CL extract. (A) HCD/UVPD of moiety PA 32:1 (dioxolane *m/z* of 571.47) results in fragment ions in agreement with (B) 16:0/16:1 dioxolane structure. (C) HCD/UVPD of moiety PA 33:1 (dioxolane *m/z* of 585.48) results in fragment ions in agreement with (D) 16:0/17:1 dioxolane structure. Selected precursor ions are demarcated with a star. MS^2 HCD of *m/z* 1413.98 is shown in **Figure S8A**.

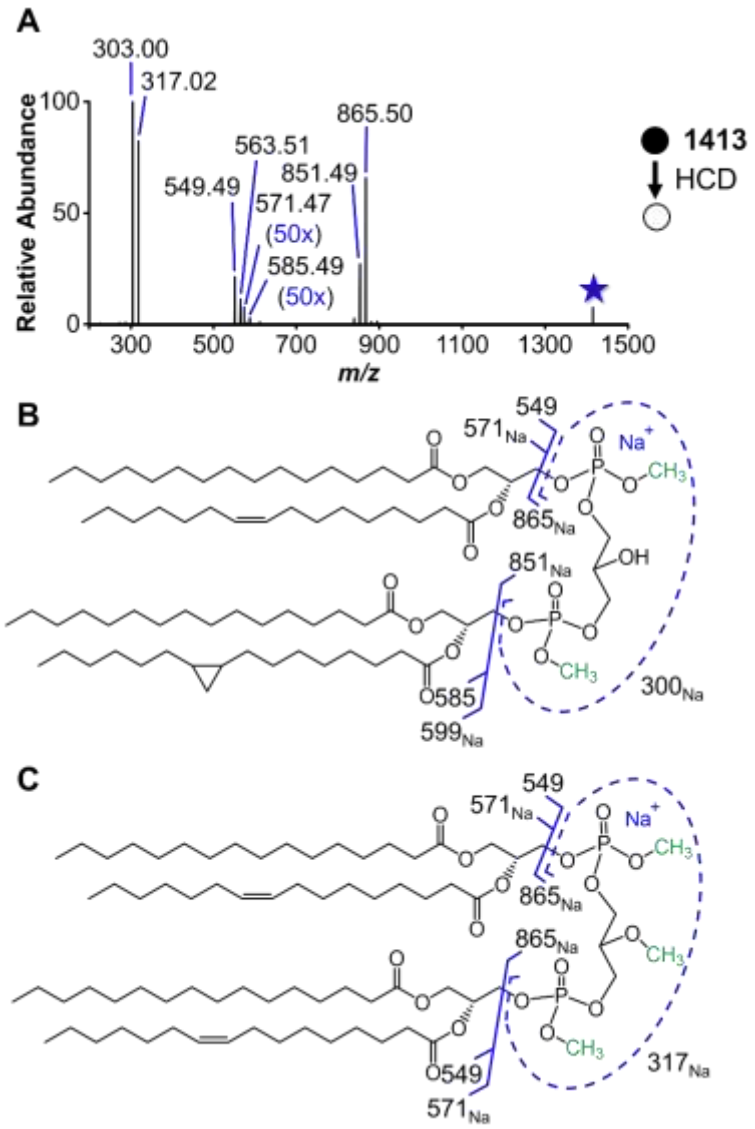

Figure S8. (A) HCD (25 NCE) spectrum of *m/z* 1413.98 from methylated *E. coli* CL extract. Selected precursor is designated with a star. Fragment ions of *m/z* 563.51 and *m/z* 585.49 are shown with 50x magnification. Fragment maps for (B) methylated CL (16:0/16:1)_(16:0/17:1) and (C) overmethylated CL (16:0/16:1)_(16:0/16:1) are shown.

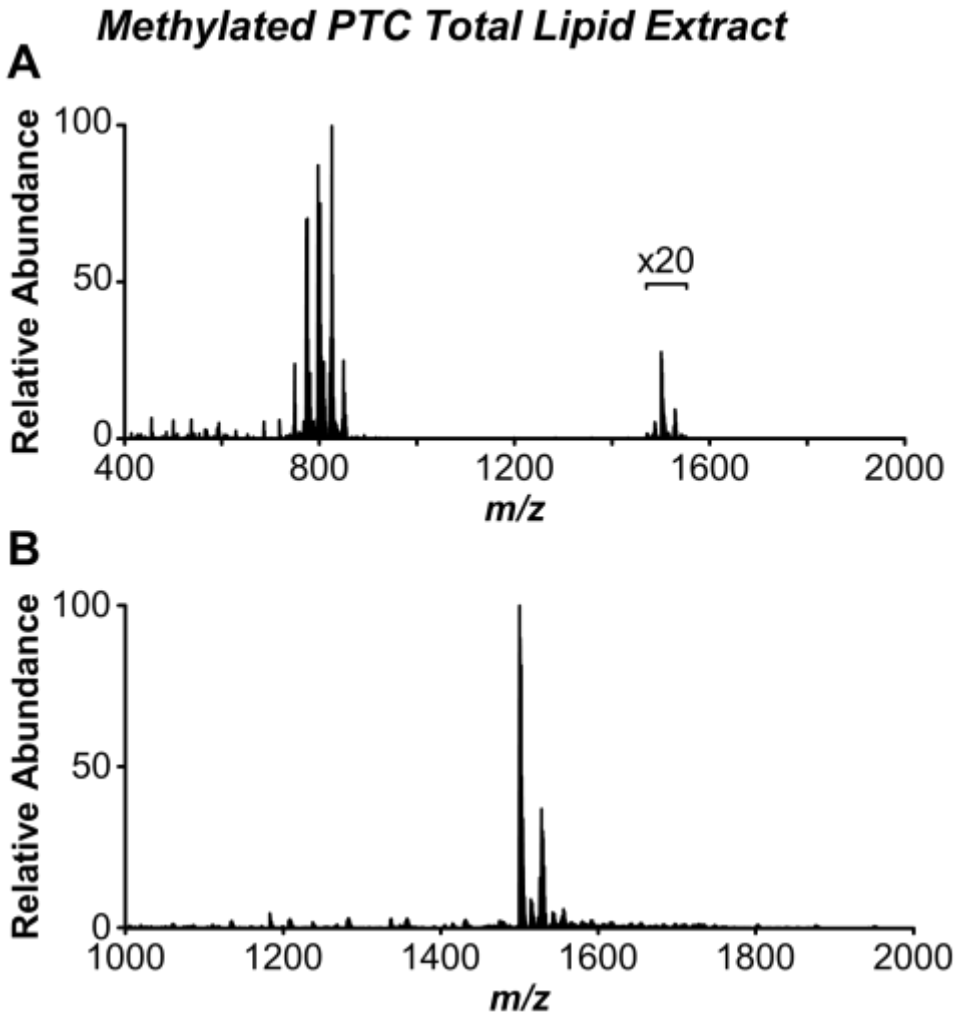

Figure S9. Positive mode MS^1 spectrum of methylated PTC total lipid extract ionized from solution doped with sodium acetate. (A) Scan from *m/z* 400-2000, with 20x magnification of CLs present in 1400-1600 *m/z* range. (B) Scan of *m/z* 1000 – 2000, showing predominance of CL species in this mass range.

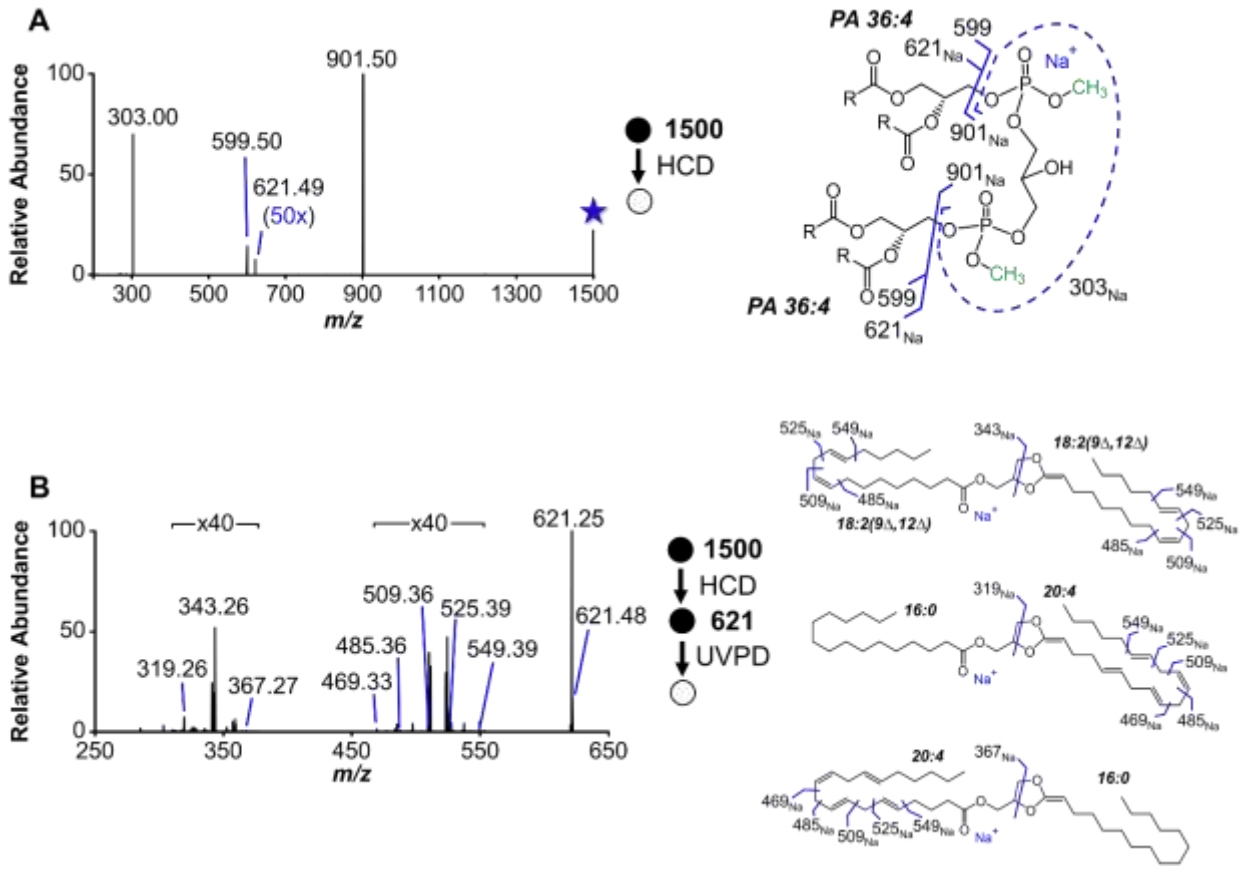

Figure S10. (A) HCD (25 NCE) spectrum and fragment map of *m/z* 1500.00 from methylated PTC total lipid extract. Selected precursor is designated with a star. Fragment ion at *m/z* 621.49 is shown with 50x magnification. (B) MS^3 UVPD (10 pulses at 3 mJ) of *m/z* 621.49 and corresponding fragment maps for 18:2(9Δ,12 Δ)/18:2(9Δ,12 Δ), 16:0/20:4, and 20:4/16:0 dioxolane structures. Ion at *m/z* 621.25 was co-isolated with precursor of *m/z* 621.49.

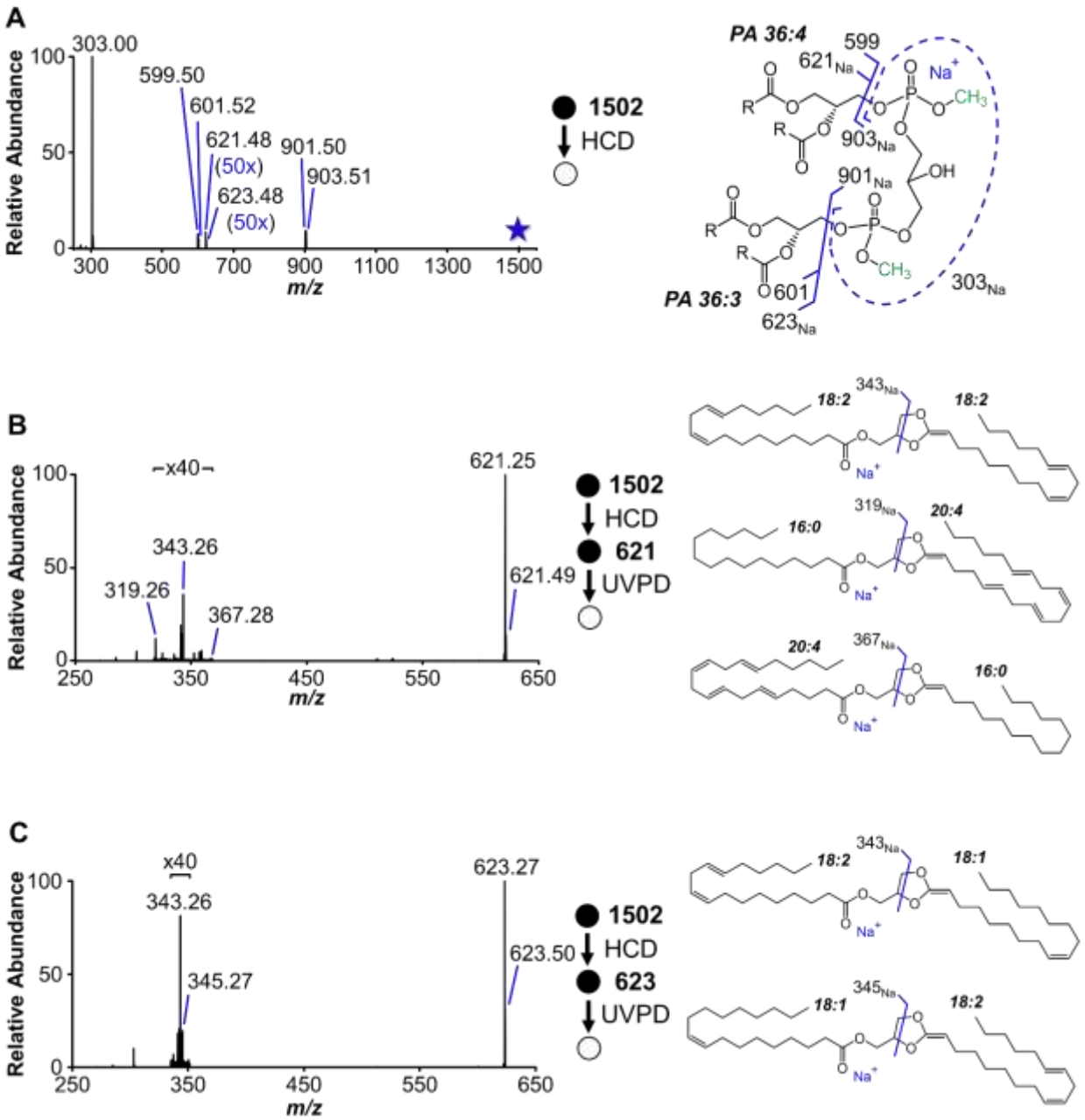

Figure S11. (A) HCD (25 NCE) spectrum and fragment map of *m/z* 1502.01 from methylated PTC total lipid extract. Selected precursor is designated with a star. Fragment ions of *m/z* 621.48 and *m/z* 623.48 are shown with 50x magnification. (B) MS^3 UVPD (10 pulses at 3 mJ) of *m/z* 621.48 and corresponding fragment maps for 18:2/18:2, 16:0/20:4, and 20:4/16:0 dioxolane structures. Ion at *m/z* 621.25 was co-isolated with precursor of *m/z* 621.49. (C) MS^3 UVPD (10 pulses at 3 mJ) of *m/z* 623.48 and corresponding fragment maps for 18:1/18:2 and 18:2/18:1 dioxolane structures. Ion at *m/z* 623.27 was co-isolated with precursor of *m/z* 623.48.

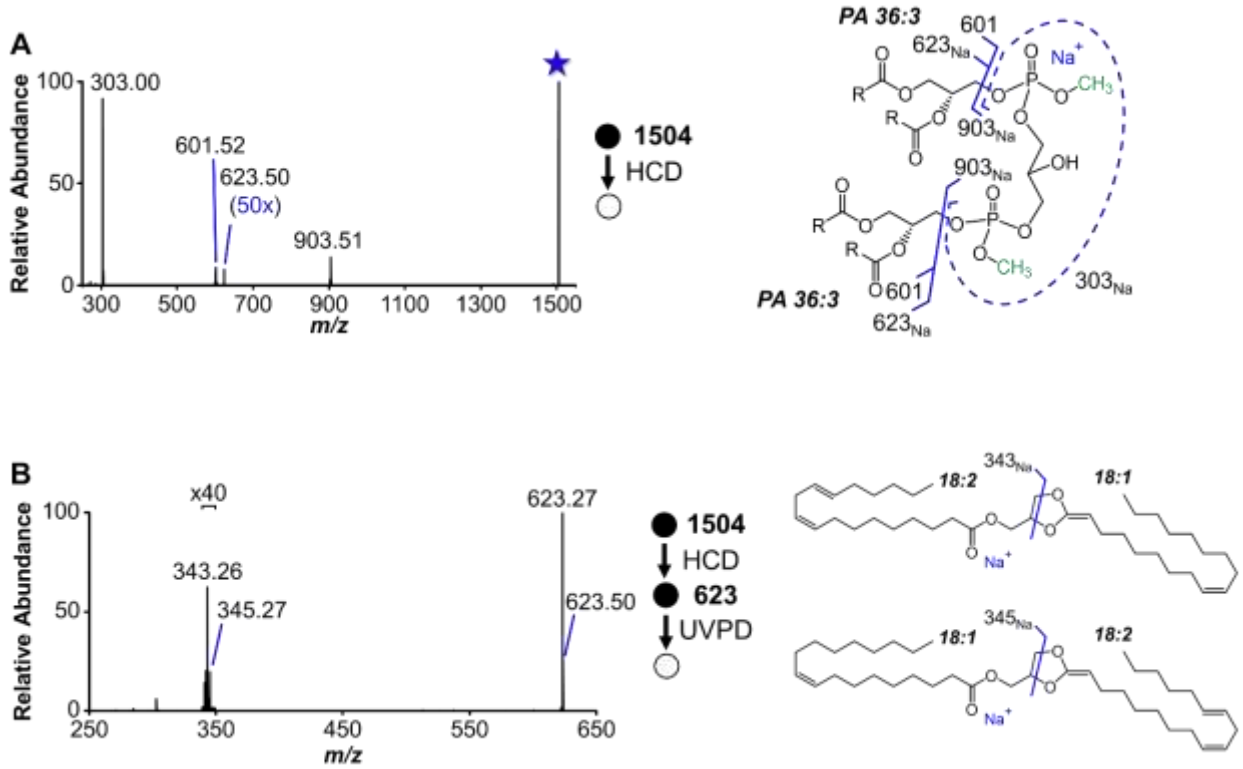

Figure S12. HCD (25 NCE) spectrum and fragment map of *m/z* 1504.02 from methylated PTC total lipid extract. Selected precursor is designated with a star. Fragment ion at *m/z* 623.50 is shown with 50x magnification. (B) MS^3 UVPD (10 pulses at 3 mJ) of *m/z* 623.50 and corresponding fragment maps for 18:2/18:2 and 18:2/18:1 dioxolane structures. Ion at *m/z* 623.27 was co-isolated with precursor of *m/z* 623.50.

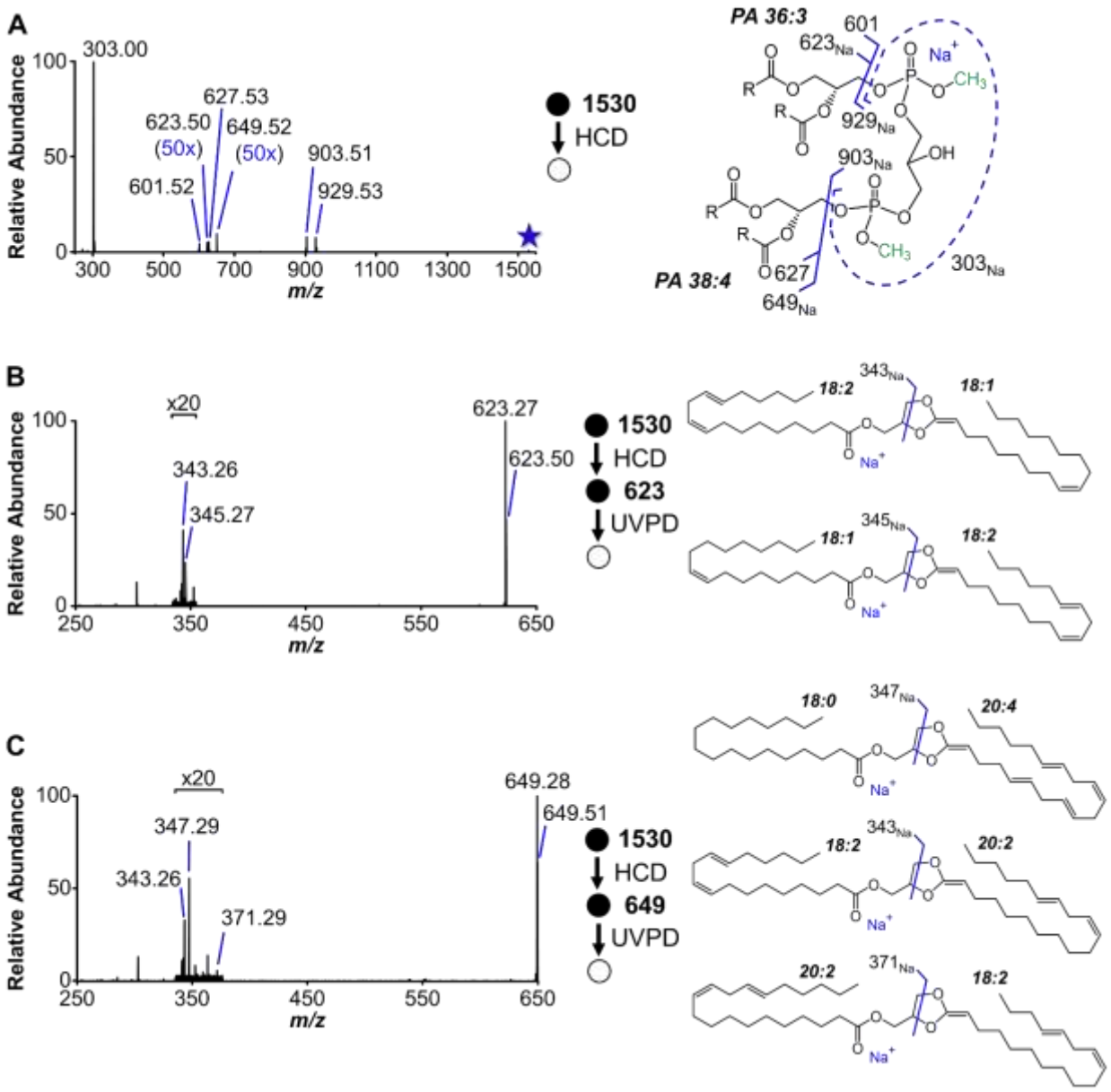

Figure S13. (A) HCD (25 NCE) spectrum and fragment map of *m/z* 1530.04 from methylated PTC total lipid extract. Selected precursor is designated with a star. Fragment ions of *m/z* 623.50 and *m/z* 649.52 are shown with 50x magnification. (B) MS^3 UVPD (10 pulses at 3 mJ) of *m/z* 623.50 and corresponding fragment maps for 18:2/18:1 and 18:1/18:2 dioxolane structures. Ion at *m/z* 623.27 was co-isolated with precursor of *m/z* 623.50. (C) MS^3 UVPD (10 pulses at 3 mJ) of *m/z* 649.52 and corresponding fragment maps for 18:0/20:4, 18:2/20:2, and 20:2/18:2 dioxolane structures. Ion at *m/z* 649.28 was co-isolated with precursor of *m/z* 649.52.

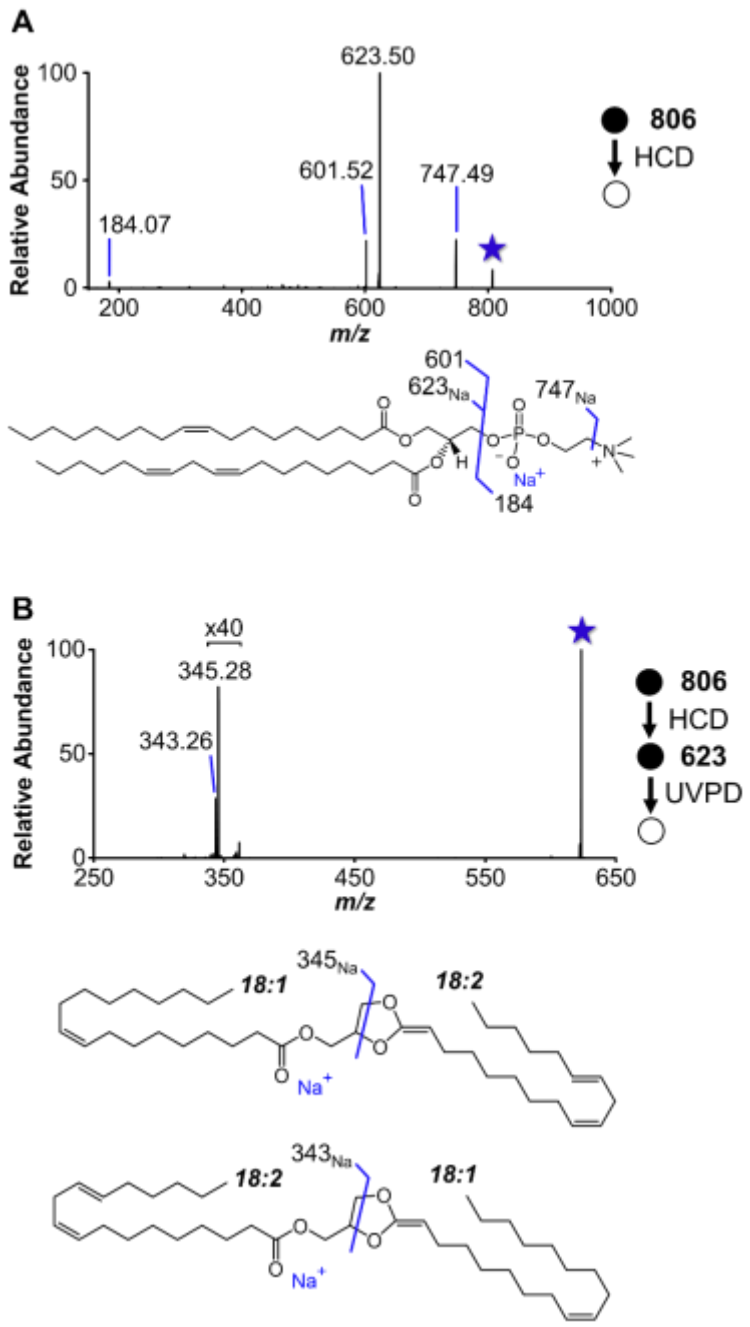

Figure S14. (A) HCD (30 NCE) spectrum and fragment map of *m/z* 806.57 from underivatized PTC total lipid extract, corresponding to sodium adducted PC 36:3. (B) MS^3 UVPD (10 pulses at 3 mJ) of *m/z* 623.50 and corresponding fragment maps for 18:2/18:1 and 18:1/18:2 dioxolane structures. Each selected precursor ion is demarcated with a star.

Supplementary References

(1) Bligh, E. G.; Dyer, W. J. A Rapid Method of Total Lipid Extraction and Purification. *Can. J. Biochem. Physiol.* **1959**, *37*, 911–917.

(2) Xia, T.; Ren, H.; Zhang, W.; Xia, Y. Lipidome-Wide Characterization of Phosphatidylinositols and Phosphatidylglycerols on CC Location Level. *Analytica Chimica Acta* **2020**, *1128*, 107–115.

(3) Lee, J. C.; Yang, J. S.; Moon, M. H. Simultaneous Relative Quantification of Various Polyglycerophospholipids with Isotope-Labeled Methylation by Nanoflow Ultrahigh Performance Liquid Chromatography-Tandem Mass Spectrometry. *Anal. Chem.* **2019**, *91*, 6716–6723.

(4) Lee, J. C.; Byeon, S. K.; Moon, M. H. Relative Quantification of Phospholipids Based on Isotope-Labeled Methylation by Nanoflow Ultrahigh Performance Liquid Chromatography–Tandem Mass Spectrometry: Enhancement in Cardiolipin Profiling. *Anal. Chem.* **2017**, *89*, 4969–4977.

(5) Cai, T.; Shu, Q.; Liu, P.; Niu, L.; Guo, X.; Ding, X.; Xue, P.; Xie, Z.; Wang, J.; Zhu, N.; Wu, P.; Niu, L.; Yang, F. Characterization and Relative Quantification of Phospholipids Based on Methylation and Stable Isotopic Labeling. *J Lipid Res* **2016**, *57*, 388–397.

(6) Liebisch, G.; Vizcaíno, J. A.; Köfeler, H.; Trötzmüller, M.; Griffiths, W. J.; Schmitz, G.; Spener, F.; Wakelam, M. J. O. Shorthand Notation for Lipid Structures Derived from Mass Spectrometry. *J Lipid Res* **2013**, *54*, 1523–1530.

(7) Macias, L. A.; Feider, C. L.; Eberlin, L. S.; Brodbelt, J. S. Hybrid 193 Nm Ultraviolet Photodissociation Mass Spectrometry Localizes Cardiolipin Unsaturations. *Anal. Chem.* **2019**, *91*, 12509–12516.

(8) Hsu, F.-F.; Turk, J. Electrospray Ionization with Low-Energy Collisionally Activated Dissociation Tandem Mass Spectrometry of Glycerophospholipids: Mechanisms of Fragmentation and Structural Characterization. *J Chromatogr B Analyt Technol Biomed Life Sci* **2009**, *877* (26), 2673–2695.

(9) Kirschbaum, C.; Greis, K.; Polewski, L.; Gewinner, S.; Schöllkopf, W.; Meijer, G.; von Helden, G.; Pagel, K. Unveiling Glycerolipid Fragmentation by Cryogenic Infrared Spectroscopy. *J. Am. Chem. Soc.* **2021**, *143* (36), 14827–14834.